SRNA – MONTE CARLO CODES FOR PROTON TRANSPORT SIMULATION IN COMBINED AND VOXELIZED GEOMETRIES

by

Radovan D. ILIĆ[1], Darko LALIĆ[2], Srboljub J. STANKOVIĆ[1]

Received on July 24, 2002; accepted in revised form on November 20, 2002

This paper describes new Monte Carlo codes for proton transport simulations in complex geometrical forms and in materials of different composition. The SRNA codes were developed for three dimensional (3D) dose distribution calculation in proton therapy and dosimetry. The model of these codes is based on the theory of proton multiple scattering and a simple model of compound nucleus decay. The developed package consists of two codes: SRNA-2KG and SRNA-VOX. The first code simulates proton transport in combined geometry that can be described by planes and second order surfaces. The second one uses the voxelized geometry of material zones and is specifically adopted for the application of patient computer tomography data. Transition probabilities for both codes are given by the SRNADAT program. In this paper, we will present the models and algorithms of our programs, as well as the results of the numerical experiments we have carried out applying them, along with the results of proton transport simulation obtained through the PETRA and GEANT programs. The simulation of the proton beam characterization by means of the Multi-Layer Faraday Cup and spatial distribution of positron emitters obtained by our program indicate the imminent application of Monte Carlo techniques in clinical practice.

Key words: proton multiple scattering, particles emission from compound nuclei decay, 3D Monte Carlo proton transport, CT data conversion and usage in proton therapy planing, proton beam characterization by Faraday Cup

INTRODUCTION

There is increasing evidence that Monte Carlo based programs are the most powerful tool in nuclear particles transport calculations. A growing number of medical physicists believe that, in the future, routine dose calculation will be performed using Monte Carlo methods [1, 2], which will prove to be dominant vehicles for dose computation in radiotherapy treatment planning [1]. The most powerful feature of the Monte Carlo method is the possibility of simulating all individual particle interactions in three dimensions and performing numerical experiments with preset errors. These facts were the motivation behind the development of the general-purpose Monte Carlo program SRNA for proton transport simulation. Some of the applications of the SRNA program are: (a) proton therapy, (b) design of accelerator driven systems, (c) radioisotopes production for medical applications, (d) simulation of proton scatterer and degrader shapes and composition, and (e) radiation protection on accelerator installations. A wide range of SRNA code applications has required the development of the SRNA-2KG code and the SRNA-VOX code. The first one is intended for proton transport simulations in technical systems described by standard geometrical forms (sphere, cone, cylinder, cube). The second was designed for radiotherapy calculations of deposited energy distribution in in-patients on the basis of computer tomography (CT) data. Both codes are capable of using 3D proton sources with an arbitrary energy spectrum within an interval of 100 keV to 250 MeV, while transition prob-

Scientific paper
UDC: 519.876.5:539.125.4
BIBLID: 1451-3994, *17* (2002), 1–2, pp. 27–36

Authors' addresses:
[1] VINČA Institute of Nuclear Sciences
P. O. Box 522, 11001 Belgrade, Yugoslavia
[2] Military Medical Academy
Crnotravska 19, 11000 Belgrade, Yugoslavia

E-mail address of corresponding author:
rasa@vin.bg.ac.yu (R. D. Ilić)

abilities are obtained through the SRNADAT program. In the first part of this paper, a description of a common model of proton transport for both codes is presented. Further on, the results of numerical experiments performed by the SRNA-2KG code are compared with the results of well known GEANT and PETRA programs. A good agreement of all said results was demonstrated. Deposited energy distribution for a 65 MeV proton beam irradiation of the patient's eye, as calculated by SRNA-VOX, is presented in several CT slices. For the purpose of simulating a therapeutic proton beam characterization by the Multi-Layer Faraday Cup (MLFC), the SRNA-2KG program was used at the Indiana University Cyclotron Facility (IUCF). An excellent coincidence between measured and simulated results has demonstrated the good features of the MLFC as a measuring device. By adding the cross section of the positron emitter creation, the same program has enabled the Brookhaven National Laboratory to simulate the spatial distribution of these emitters a step ahead of the estimation of proton dose distribution by positron emission tomography. The said programs are written in Fortran 77, run on PC and are distributed on a single floppy disk.

PROTON TRANSPORT MODEL

The simulation of proton transport is based upon the multiple scattering theory of charged particles [3, 4, 5], energy losses with fluctuation [6, 7] and our model of compound nucleus decay simulation after proton absorption in nonelastic nuclear interactions.

Energy losses, proton step and energy scale

In order to simulate proton transport, the proton trajectory is divided into small steps, whose length Δs is determined by a small energy loss ΔE

$$\Delta s = \int_{E_{n+1}}^{E_n} \frac{dE}{(dE/dx)_{tot}} \qquad (1)$$

Energy loss $\Delta E = E_n - E_{n+1}$ is chosen to be several percents of the initial proton energy. The conditions for the implementation of the multiple scattering theory and the calculation of energy loss with its fluctuations demand that the energy scale be partially linear and partially logarithmic. Energy E_{pek}, which splits the energy scale into a linear and a logarithmic part, can be arbitrarily chosen. The PTRAN [8] program model shows that the best results are obtained with E_{pek} amounting to about 10 MeV. The volume and the quality of energy and angular distributions are determined by the energy scale choices. According to our experience, the best energy scale is obtained with ΔE_{av} average energy loss at about $0.05\,E_{pek}$. Stopping power (dE/dx) can be obtained from ICRU49 [9], or calculated according to the Ziegler empirical formulae [9].

After the energy scale is prepared, it is necessary to modify it. Firstly, the average number of collisions on step Δs must be greater than the minimal value ($\Omega_0 > 10$), according to the multiple scattering theory conditions. Secondly, Vavilov's parameter κ must be lesser than the maximal value ($\kappa < 20$). After a few iterations, both conditions can be met and the energy scale definitely prepared for the calculation of proton transition probabilities.

Energy loss fluctuation

Usually, the probability density function and distribution functions are calculated in the following order: the probability density function first and after that, the density function is calculated from the probability density function. The SRNA code uses another approach [10] whereby the distribution function is directly calculated. The starting point of our calculations is the function given by Vavilov in the following form [6]:

$$f(\Delta s, \Delta) = \frac{1}{\pi\xi}\kappa \exp[\kappa(1+\beta^2 C]\cdot$$
$$\cdot\int_0^\infty \exp(\kappa f_1)\cos(y\lambda + \kappa f_2)dy$$

$$f_1 = \beta^2[\ln y - Ci(y)] - \cos y - ySi(y) \qquad (2)$$

$$f_2 = y[\ln y - Ci(y)] + \sin y + \beta^2 Si(y)$$

$$\kappa f_1 \Rightarrow \kappa(f_1 - y^2 D/\varepsilon_{\max})$$

$\lambda = (\Delta - \Delta_{av})/\xi + \lambda_{av}$ denotes the distribution parameter, Δ – probable energy loss, and Δ_{av} – average energy loss. The other terms in (2) have the following meaning:

$$\xi = 2\pi {r_e}^2 m_e c^2 \rho N_a \frac{\Delta s}{\beta^2}\sum_j w_j \frac{Z_j}{A_j}$$

$$\lambda_{av} = -1 + C - \beta^2 - \ln\kappa \qquad (3)$$

$$\kappa = \xi/\varepsilon_{\max} \quad \varepsilon_{\max} = \frac{2m_e c^2\beta^2}{1-\beta^2}$$

where ρ is density, N_a – Avogadro's number, r_e – clasical electron radius, m_e – electron rest mass, Z_j, A_j, and w_j are atomic number, atomic weight, and weight fraction of the j^{th} constituent, Δs – proton step, $C = 0.5772156649\ldots$ is Euler's constant, ε_{max} is the maximum amount of energy which a proton can lose with a free orbital electron, $Si(x)$ and $Ci(x)$ are integral sine and cosine, and D is Shulek's correction [7]

$$D = \frac{4}{3}\sum_n I_n g_n \ln(2m_e c^2\beta^2 / I_n) \qquad (4)$$

for the influence of electron orbits on the distribution. In (4) I_n is the excitation potential of the electron orbit and g_n is the ratio of the number of orbital electrons to the total number of electrons.

In order to calculate the distribution function, eq. (2) should be first integrated over λ. So, obtained function is transformed in form suitable for numerical integration by the Gauss-Kronrod algorithm. The choice of integration limits over y and step depends on the characteristics of this function. The quality of the integration is estimated by the following numerical parameters: absolute error equal to 10^{-7}, relative error equal to 10^{-6} and distribution normalization onto 0.999999. Under these conditions $y_{max} = 100$ and λ takes a value between –5 and 35.

Vavilov's distribution function obtained in this way is shown in Fig. 1. Shulek's correction has effect in the case of higher atomic numbers causing the spread of distribution. It is necessary to calculate at least 256 values of inverse distribution using approximation with cube spline.

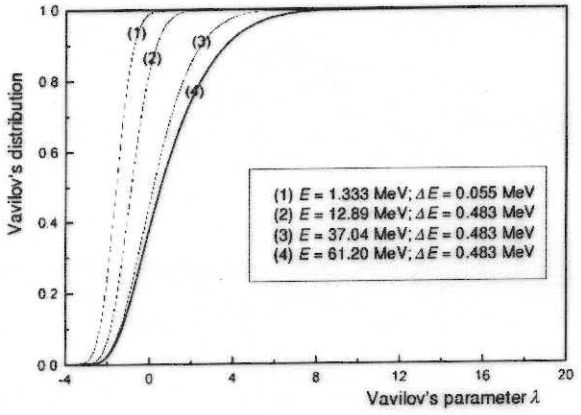

Figure 1. Vavilov's distribution function of fluctuation of average energy loss in water

Proton angular distribution

The angular distribution of multiple scattered protons was obtained through the integration of Moliere's density function. This density function is derived in form of order [4, 5] with parameter B-ln(B) = ln(Ω) where Ω denotes the average number of collisions on step Δs

$$F(\vartheta) = \frac{1}{\chi_c\sqrt{B}}\sum_n \int_0^{\vartheta} d\varphi \frac{f_n(\varphi)}{B^n}\varphi \qquad (5)$$

In eq. (5) $\vartheta = \theta / \chi_c\sqrt{B}$ denotes a reduced angle and $f_n(\varphi)$ are Moliere's functions given by:

$$f_m(\varphi) = \frac{1}{m!}\int_0^{\infty} dy\left[\frac{y^2}{4}\ln\frac{y^2}{4}\right]^m J_0(\varphi y)\exp\left(-\frac{y^2}{4}\right) \qquad (6)$$

For compound materials, the Moliere screening angle is given by:

$$\chi_c = 4\pi N_a\left[r_e\frac{m_e}{M}\frac{\tau+1}{\tau(\tau+2)}\right]^2\sum_j w_j\frac{Z_j^2}{A_j}\Delta s \qquad (7)$$

In (7) N_a denotes Avogadro number, r_e and m_e are the classical radius and rest mass of electron, M is the mass of the proton, $\tau = E_k/Mc^2$ is the reduced kinetic energy of the proton, w_j the weight fraction of element Z_j and atomic weight A_j, and Δs is the proton step. We have calculated functions (6) in the interval $0 \le \varphi \le 40$ by using the Gauss-Kronrod algorithm again. Inverse Moliere distributions were calculated similarly to Vavilov's inverse distributions. Angular proton distributions for 4 values of proton energy E, are shown in Fig. 2.

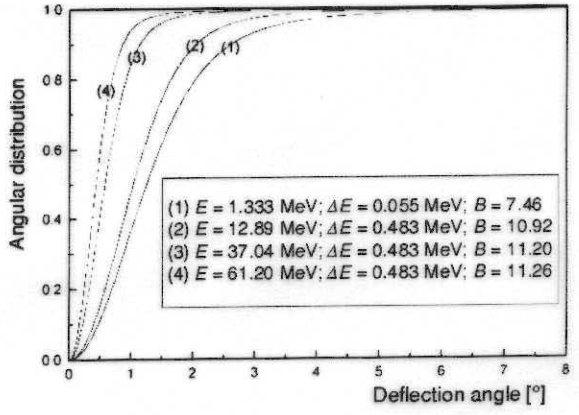

Figure 2. Angular distributions of multiple scattered protons in water

Nonelastic nuclear interactions

Nonelastic nuclear interactions are rare events, but they are very important for the correct modeling of proton transport. In order to simulate nonelastic nuclear interactions in materials, the cross sections of all constitutive elements of these materials must be known. For a limited number of elements, these cross sections [11] are available in the energy range from the threshold to 150 MeV, and in ICRUTAB [9, 12] up to 250 MeV. Judging by current trends in the development of therapy planning tools based on the Monte Carlo technique, we can expect the expanding of the cross section data.

Using available data, we established a model for nonelastic nuclear reaction simulation and for secondary particle emission. That model has the following steps: (1) determination if the nonelastic reaction event occurs, (2) selection of a nucleus with which a proton interacts and energy is transferred to the nucleus, (3) probable number of secondary particles, and (4) energy and angle of the secondary particles emitted. For every single step, we need the distribution described here.

Average number of nonelastic nuclear interactions

The average number of interactions on proton step Δs is calculated according to the following relation:

$$q(E) = \rho \frac{N_a}{A} \int_{E_{n+1}}^{E_n} \sigma(E) \frac{dE}{(dE/dx)} \qquad (8)$$

where ρ is the density, N_a is Avogadro's number, A is atomic weight, $\sigma(E)$ is the nonelastic nuclear interaction cross section, and dE/dx is the total stopping power. Figure 3 shows the average number of nonelastic nuclear interactions with the proton in ^{16}O.

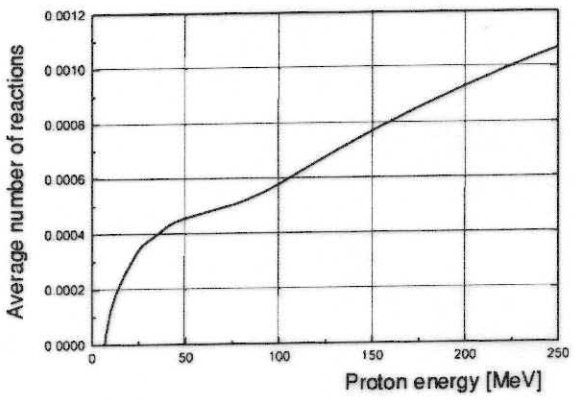

Figure 3. The average number of nonelastic proton interactions in ^{16}O

Probable nucleus of interaction and its recoil energy

The probable nucleus j with which a proton will enter into a nonelastic nuclear reaction is determined by the discrete cumulative distribution $P_j = \sum_{i=1}^{m} p_i$ where $p_i = (g_i\sigma_i)/(\sum_{k=1}^{m} g_k\sigma_k)$ are the probabilities for nucleus i whose weight contribution is g_i; m is the total number of nuclei within the material. ICRUTAB [9] data contain the values of recoil energy E_{ric} par nonelastic nuclear reactions of the proton with that nucleus. If the energy of the proton was E_p before a reaction, the created compound nucleus occurs with energy $E_p - E_{ric}$, and energy E_{ric} is deposited at the site of the reaction.

Secondary particle emission

When a compound nucleus is created, according to Chadwick's model, it will decay by simultaneous emission of neutrons, protons, deuterons, tritons, alpha-particles and photons. For every single particle emitted, a mean multiplication factor F_m exists in the ICRUTAB data. If we accept that for such rare events Poisson's distribution is adequate, we can determine the probable number of particles emitted for every single type of particle. Such a model demands that for every single type its probable number of secondary particles must be found, even in the case when F_m is of a very small magnitude. Our model of compound nucleus decay simulation comprises all possible combinations of emission for all of the six secondary particles mentioned above and for each proton energy.

Energy and angle of secondary particles

From the double differential cross section one can obtain the energy and angular distribution by a common procedure for numerical integration. In our model, we have used the energy spectrum already prepared in ICRUTAB for inverse energy distribution calculations, as the one used in the case of Vavilov's and Moliere's distributions. In this way, we have made easier the procedure for angular distribution determination, which also is inverted in the same manner. For a type of secondary particles given in advance, with energy E_p, from inverted distribution, one can choose the energy of that particle E_{sp} and the angle of its emission ω_{sp}. For every single type of secondary particles, one has to check if the sum $\sum_{n=1}^{N} (E_{sp})_n$ of energies of the secondary particles N is less or equal to proton energy E_p. When that sum is greater then the proton energy, N-1 addend has to be subtracted and compound nucleus decay simulation terminates. The mean value of the remaining proton energy is very close to the q value of the reaction. In the TERA project,

the 250 MeV proton transport simulation in a tissue equivalent phantom was performed with GEANT and LAHET codes. In these simulation, an average deposited energy is 232.83 ± 4.3 MeV, with a cut in energy of 10 MeV. The SRNA-2KG simulation, in some phantoms, with a cut in energy of 100 keV, gives 226 ± 7.4 MeV.

Only secondary protons are included in the transport simulation model, while deuterons, tritons and alpha particles are deposited on the spot. Neutrons and photons are not included in the said transport model. They are registered in the data file where each line contains: the index of the particle, energy, (x, y, z)-coordinates, sine and cosine of polar and azimuthal angles. This data file can be used by the MCNP4B program [13] in order to simulate neutron and photon transport or by FOTELP [14] and PENELOPE [15] programs to simulate photon transport only.

Change of proton direction

At the end of each proton step, the direction of the proton changes. This change of direction is specified in terms of polar ϑ' and azimuthal φ' angles, within a coordinate system whose polar axis coincides with the direction of the motion of the proton at the beginning of the step. The polar angle is sampled from Moliere's distribution, the azimuthal angle from an uniform distribution in 2π. Direction cosines at the end of the proton step are usually calculated according to Berger's model [3].

Change of proton position

The coordinates of a proton after passing step Δs within the local coordinate system are given by Berger [8]

$$\Delta x = \frac{\Delta s}{2}[\sin\vartheta' \cos\varphi' + \gamma_x(\theta_{av}^2/6)^{1/2}]$$

$$\Delta y = \frac{\Delta s}{2}[\sin\vartheta' \sin\varphi' + \gamma_y(\theta_{av}^2/6)^{1/2}] \qquad (9)$$

$$\Delta z = \frac{\Delta s}{2}(1+\cos\vartheta')$$

where ϑ' and φ' are polar and azimuthal angles and $\theta_{av}^2 = \chi_c^2(B-1.2)$ is the approximation of the mean-square multiple scattering deflection.

Position of the event along the step

On step Δs, a proton can lose energy ΔE, or be absorbed in nonelastic nuclear interactions. Density functions along the step of these events are unknown. We assumed an uniform distribution of these events. This is more realistic than the usual assumption that these events take place at the end of a proton step.

Borderline between zones

The lengths of proton steps Δs_m are calculated in advance according to (1) for each material. In some cases, the length of a proton step may be larger than the distance L to the zones borderline, calculated in the direction of proton transport. In the nearest material, the proton step and other condensed history proton parameters have different values. Because of it, we have focused on solving the problems on the borderline between the zones in the easiest way, *i. e.*, without an increase in simulation time or significant perturbations of the physical process picture. In the SRNA codes, energy loss ΔE_m on step Δs_m was multiplied by the factor $L/\Delta s_m$ in order to obtain the deposited energy in the current zone only if $L < \Delta s_m$. After that, the proton starting point has moved to the zones borderline. The deflection angle was sampled from appropriate, previously prepared distribution (5).

Geometry

Transport simulation of particles is limited by the geometrical description of the transport medium. Real geometrical shapes of technical systems may be described by planes and second order surfaces, as in RFG [21] or PENGEOM and PENELOPE [15] programs, and fourth order surfaces in MCNP4B [13]. For describing patient geometry, standard shapes are usually applied. This is only a crude approximation, because it is a technical description of a patient's geometry. The most accurate way of describing the patient's geometry is by means of CT data [1, 16]. CT data permit 3D transport simulation, including variations of tissue densities and compositions. Using the same proton transport model, we developed two versions of the SRNA program. The first version of our code uses RFG or PENGEOM programs as geometrical models. The second, voxelized version, is adjusted to CT data. Only in this version, the routine GEMVOX with heightened calculation speed for estimating the distance from proton position within the voxel to its nearest plane has been developed.

Conversion of Houndsfield's numbers to density

The dimension and number of voxels along with Houndsfield's numbers are the basis for the preparation of simulation data. The main problems due to the determination of density and elemental composition of the patient's tissue on the basis of CT data are described [16]. In our model, in order to spare computer memory, the intervals of

Houndsfield's numbers are associated with elemental tissue composition and its densities.

By applying the DICOM standard, we are able to distinguish Houndsfiedls's numbers and to convert them into an integer matrix MH (i,j,k), where (i,j,k) represent the voxel index. Its contents, presented on the screen, enable us to select, in a natural way, the types of tissues that surround a tumor, as well as Houndsfiels's numbers that correspond to them. In tissues selected in this manner, we join the density and limits around the mean values of Houndsfield's number from its interval (H_l, H_{l+1}). That approach was used in creating data shown in Table 1. The preparation of CT parameters for better simulation was reduced to the conversion of the density of each voxel to matrix $MG_n\ (i, j, k) = 10000\ \rho_n\ [MH\ (i, j, k)]$ for every single tissue (material) from 1 to N. For all other materials, we prepared the transition probabilities and other constants necessary for the simulation without repetition. Every single material gets its own identification 10000 ρ_n, by which we recognize the type of material being in the voxel. Whenever, with the help of the anatomical picture, we found that we got a different Houndsfields's number for the same tissue, in such a case, the tissue retained its natural elementary structure and every tissue its own density. In such cases, our program treated identical materials of different densities as different materials.

Table 1. Intervals of Houndsfield's numbers with average densities and tissue composition according to the available data prepared by Scheinder [16]: *Mat* – tissue; H_{nd} – Houndsfield's number, ρ – density [g/cm^3]

Mat	H_{nd}	ρ	H	C	N	O	P	Ca
1	–950	Air						
2	–741	0.26	10.3	10.5	3.1	74.3	0.2	
3	–98	0.93	11.6	68.1	0.2	19.8		
4	–77	0.95	11.4	59.8	0.7	27.8		
5	–55	0.97	11.2	51.7	1.3	35.5		
6	–49	0.98	11.5	64.4	0.7	23.1		
7	–22	1.00	11.0	52.9	2.1	33.5	0.1	
8	–1	1.02	10.6	33.2	3.0	52.8	0.1	
9	11	1.03	10.5	41.4	3.4	43.9	0.1	
10	23	1.03	10.6	11.5	2.2	75.1	0.1	0.5
11	42	1.05	10.4	11.9	2.4	74.5	0.1	0.7
12	102	1.10	9.6	9.9	2.2	74.4	2.2	
13	385	1.25	7.8	31.6	3.7	43.8	4.0	8.5
14	466	1.30	7.3	26.5	3.6	47.3	4.8	9.8
15	586	1.36	6.9	36.6	2.7	34.7	5.9	12.8
16	657	1.41	6.4	26.3	3.9	43.6	6.0	13.1
17	742	1.46	6.0	25.0	3.9	43.5	6.6	14.3
18	843	1.52	5.6	23.5	4.0	43.4	7.2	15.6
19	999	1.61	5.0	21.2	4.0	43.5	8.1	17.6
20	1113	1.68	4.6	19.9	4.1	43.5	8.6	18.7
21	1500	1.75	4.2	20.4	3.8	41.5	9.3	20.2

Proton sources

In SRNA codes, proton sources are given in the form of beams of circular and rectangular cross sections. The beams can be rotated in 4π around the irradiated object. For the purpose of accelerator simulations, it is possible to obtain a phase space file of particles on the reference surface. These files, produced by the SRNA-2KG code, contain proton energy, position and direction data in each line and can be used as a proton source similar to the emission spectra of the well-known BEAM code [17]. Both versions of the SRNA code can use phase space files as proton sources.

Scoring grid and simulation precision

In both versions of the SRNA code, a grid of rectangular elemental volumes for energy deposition scoring (MeV/kg) was used. If CT data are used for simulation, this grid is coincident with the grid of CT voxels. On the other hand, the selfsame grid is used for precision determination of energy deposition. The SRNA-2KG code calculates the precision of simulations for each material zone or appropriate separate part of the zone. The scoring grid permits precision estimation of deposited energy x_i for each elemental volume or for a group of volumes. During the simulation, values of Σx_i and Σx_i^2 are scored for each voxel or groups of elemental volumes. At the end of the simulation, precision is calculated by using these two obtained values.

NUMERICAL EXPERIMENTS

Due to limitations in cross section data for nonelastic nuclear interactions and the availability of simulation data obtained by other codes, numerical experiments were performed for water and tissue. The results of these numerical experiments for initial proton energies of 26.4, 66, 100, 205, and 250 MeV are presented here with statistical errors from 2 to 3%. Initial numerical experiments were performed by utilizing the SRNA-2KG code in order to verify the Multi-Layer Faraday Cup in the proton beam. Expanded with the cross sections of the positron emitters generation, that version of the code enables the estimation of the spatial distribution of positron emitters. The most interesting numerical experiments with protons in voxelized geometry were performed using patient CT data.

Homogenous phantom

The results of the SRNA-2KG code for the homogenous water phantom are compared with the results of PETRA [18] and GEANT [20] codes.

Comparison with LAHET and GEANT codes was done for the homogenous tissue equivalent phantom [19]. The model of PTRAN [8] code differs from our model and PETRA models in treating nonelastic nuclear interactions. When the transport of secondary protons is excluded from the SRNA code, the results of PETRA and PTRAN are coincident [18, Fig. 28] with our results in those conditions. The results in full are models shown in Fig. 4 for 26.4 MeV of proton energy and in Fig. 5 for 66 MeV of proton energy in a homogenous liquid water phantom.

A realistic picture of deposited energy changes along the depth and arrow of Bragg's peak requires a low energy cut-off. Because of this, the cut-off energy in SRNA codes is nominally set to 100 keV. These results are shown in Figs. 5 and 6. The maximum of Bragg's peak appears at a depth that agrees with the theoretical proton range. It shows that the model of proton passage is correct.

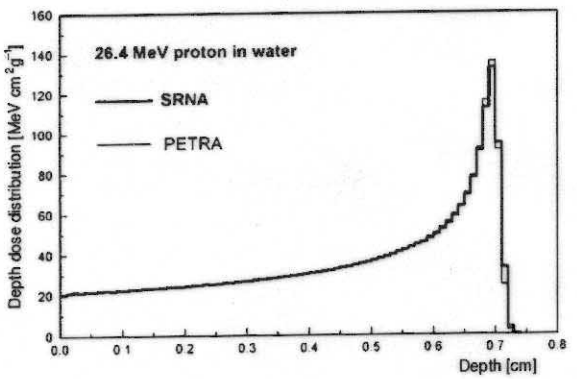

Figure 4. Monte Carlo simulation of depth dose distribution in water for 26.4 MeV protons beam

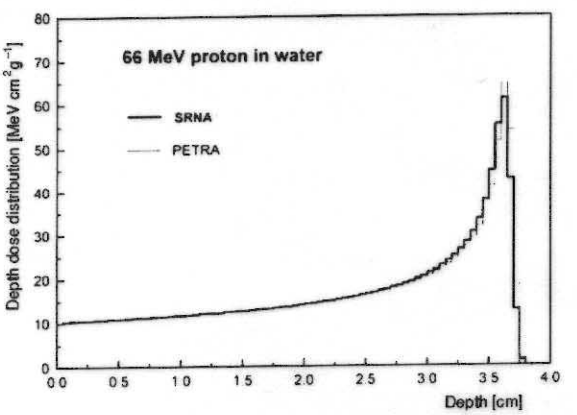

Figure 5. Monte Carlo simulation of depth dose distribution in water for 66 MeV protons beam

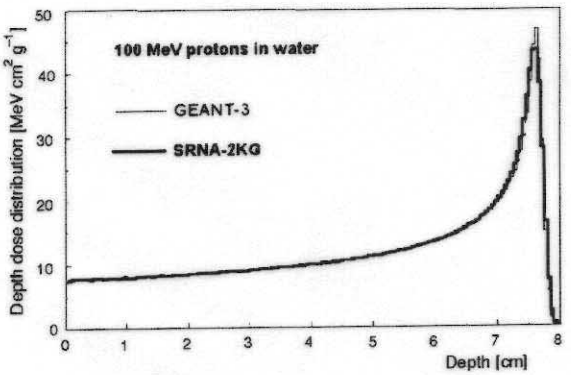

Figure 6. Monte Carlo simulation of depth dose distribution in water for a 100 MeV protons beam

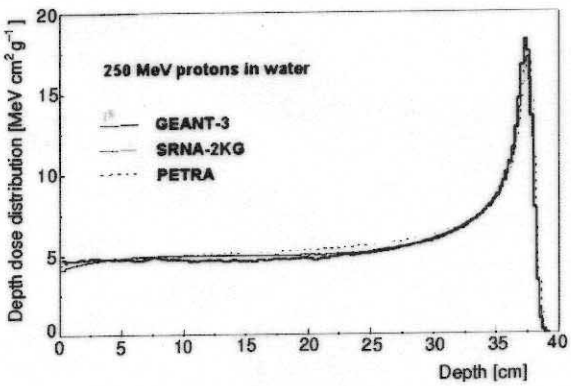

Figure 7. Monte carlo simulation of depth dose distribution in water for 250 MeV protons beam

Nonelastic nuclear interactions have little influence on energies presented above, hence their effect is not visible. As pointed out previously, these reactions, although rare, have a significant influence on the deposited energy distribution. Their increasing influence can be seen in Figs. 6 and 7.

In these figures, the results for 100 and 250 MeV proton beams in the water phantom for SRNA-2KG and GEANT codes are presented. These results illustrated the applicability of our code to higher proton energies. It should be mentioned that variations of curves for shallower depths in Fig. 7 are the results of compound nucleus decay. With increasing depth, the said effect decreases, due to an increase in ionization losses.

Voxelized geometry

In order to examine the proton transport model, two experiments were performed with a 250 MeV proton in water. Depth dose distribution was calculated with SRNA-2KG using a RFG geometrical module and with the SRNA-VOX code in

voxelized geometry. In both cases, transition probabilities were prepared with the SRNADAT code. The good agreement between both experiments shows that the previously described algorithm of the borderline between the zones is acceptable. These results are the basis of an attempt to simulate proton dose distribution in real patient geometry using CT data with pixel dimensions equaling 0.081×0.81 cm^2 and slice thickness of 0.5 cm. We assumed that a tumor is situated in the eye base. In simulation, the tumor was irradiated with a 65 MeV proton beam with a circular cross section, whose radius is 1.2 cm. The simulation was performed with 100 000 incident protons and tissue data for 21 "material" from Table 1. The deposited energy distribution in patient slices, obtained by the SRNA-VOX code, is presented in Fig. 8*.

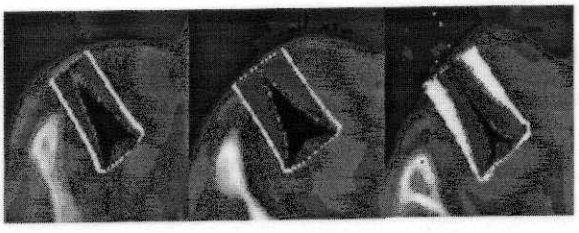

Figure 8. Deposited energy in eye slices normalized on maximum values in each slice, obtained by the SRNA-VOX code in voxelized geometry on the basis of CT data and tissue data from Table 1

* Interested readers can obtain more detailed, color pictures from the author by E-mail.

Multi-Layer Faraday cup experiments

The quality and reproducibility of the proton beam for proton therapy is very important. To obtain precise dosimetry, the beam must be calibrated according to the predetermined initial energy and acceptable energy spread. At the Indiana University Cyclotron Facility, the Multi-Layered Faraday Cup (MLFC) was used [22] to characterize the proton beam of the accelerator. Monte Carlo simulation, using SRIM, SRNA-2KG and GEANT3 programs, provided data for this project which were then compared with actual measurement data. Figure 9 shows simulated and measured data for 205 MeV proton energy with different spreads. The MLFC will resolve adequate beam characteristics for proton therapy and proper dosimetry. A simple test for the nuclear interaction model [23] can be checked by the MLFC.

Positron emitter distribution simulation

During proton therapy, in nonelastic nuclear interaction, positron emitters are created in tissue (for instance ^{11}C, ^{13}N, ^{15}O). The verification of the therapy can be achieved by comparing PET image discending the positron activity distribution with the predicted target dose distribution used to plan the treatment. For such feasibility estimation purposes, at Brookhaven National Laboratory, the SRNA-2KG program was modified by the inclusion of positron emitters cross sections, upon which their spatial distribution within the tissue was simulated at 250 MeV proton beam with a 2 mm diameter [24].

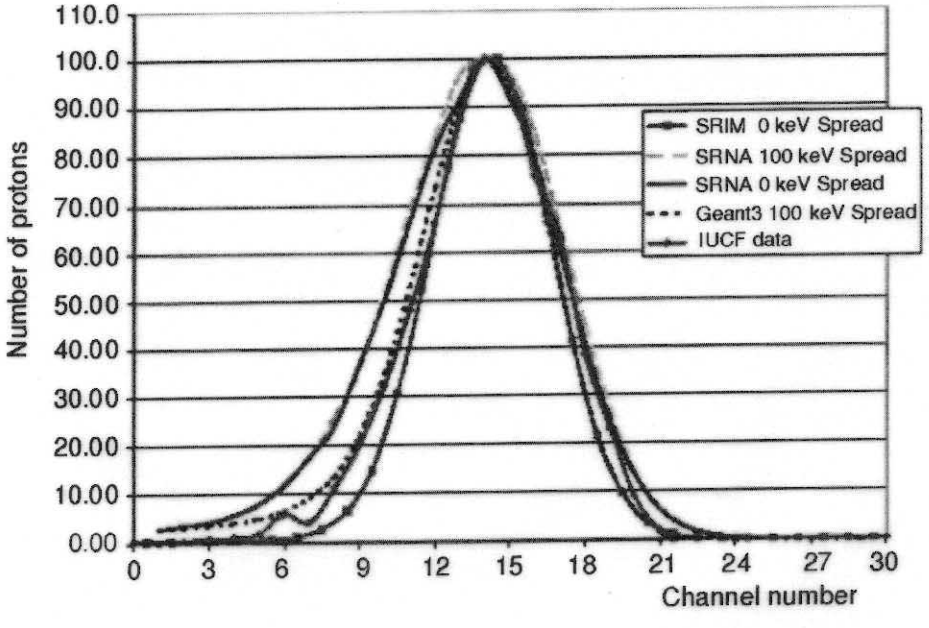

Figure 9. Number of protons stopped in Multi-Layered Faraday Cup: Monte Carlo simulation and measurement in IUCF and a 205 MeV proton beam. Channel number denotes the ordinal number of aluminum layer in MLFC

CONCLUSION

A model of the Monte Carlo SRNA code and representative numerical experiments were described here. The results of numerical experiments, in good agreement with the results of several well-known codes, show the validity of the SRNA model of proton transport simulation. In the energy range of up to 26.4 MeV, the nonelastic nuclear interactions can be neglected; up to 66 MeV, these reactions should be taken into consideration for rigorous simulation; above 66 MeV, the nonelastic nuclear interactions must be included in the simulation. Numerical experiments by the SRNA-2KG and GEANT codes and measurements show that a MLFC is a very good and simple tool for testing the nuclear interaction model and that every Monte Carlo code used in charged particle therapy should pass the MLFC test. We believe that SRNA codes have successfully passed this test and that these experiments are a demonstration of the potential feasibility of our codes in dosimetry and radiotherapy.

ACKNOWLEDGMENTS

This work is supported by the Ministry of Science, Technologies and Development of the Republic Serbia under contract No. 2016 (Physics of radiation protection).

We would like to thank Joakim Medin from the Department of Radiation Physics, Malmö University Hospital, Sweden, for help and cooperation in testing his PETRA code and comparison of these results with the results of our SRNA code simulation. We are also grateful to Mariana Bondila from the Accelerator Laboratory, University of Jyvaskyla, Finland, for careful simulation by GEANT code.

REFERENCES

[1] Sempau, J., Wilderman, S. J., Bielajew, A. F., DPM, a Fast, Accurate Monte Carlo Code Optimized for Photon and Electron Radiotherapy Treatment Planning Dose, *Phys. Med. Biol.*, *45* (2000), pp. 2263–2291

[2] Hartmann-Siantar, C. L., Bergstrom, P. M., Chandler, W, P., Chase, L., Cox, L., Daly, T. P., Garett, D., Hornstein, S. M., house, R. K., Moses, E. L., Patterson, R. W., Rathkopf, A., Schach von Witerman, A., Lawrence Livermore National Laboratory's PEREGRINE™ Project, *Proceedings*, 12th Conference on the Use of Computers in Radiotherapy, Medison, Medical Physics Publ., 1997, pp. 19–22

[3] Berger, M. J., Monte Carlo Calculation of the Penetration and Diffusion of Fast Charged Particles, in: *Methods in Computational Physics*, Vol I, Accad. Press, New York, 1963, p. 135

[4] Moliere, G., Theorie der Streuung schneller geladener Teilchen II: Mehrfach- und Vielfachstreuung, *Z. Naturforsch*, *3a*, 1948, pp. 78–97

[5] Bethe, H. A., Moliere's Theory of Multiple Scattering, *Phys. Rev.*, *89* (1953), pp. 1256–1266

[6] Vavilov, P. V., Ionizational Losses of High Energy Heavy Particle (in Russian), *J. of Phys USSR.*, *32* (1957), 4, pp. 920–923

[7] Shulek, P., Golovin, B. M., Kolyukina, L. A., Medvedev, S. N., Pavlovich, P., Fluctuation of Ionization Losses (in Russian), *J. of Nucl. Phys.*, *4* (1966), 3, pp. 564–566

[8] Berger, M. J., Proton Monte Carlo Transport Program PTRAN, 1993, Report NISTIR-5113

[9] ***, Stopping Power and Ranges for Protons and Alpha Particles, ICRU Report 49, Bathesda, USA, 1993

[10] Ilić, R. D., Vavilov's Distribution Data Preparation for Heavy Charged Particles Transport by Monte Carlo, XLIII Conf. ETRAN (in Serbian), Zlatibor September 20–22, Yugoslavia, 1998

[11] Chadwick, M. B., Data ICRUTAB.TAR from ftp://t2.lanl.gov/, 1998

[12] Young, P, G., Arthur, E. D., Chadwick, M. B., Comprehensive Nuclear Model Calculation: Theory and Use of the GNASH Code in RSICC PSR-125, ORNL TN, USA

[13] Briesmeister, J. F., MCNP – A General Monte Carlo N-Particle Transport Code, Version 4B, LA12625-M, Los Alamos National Laboratory, USA, 1997

[14] Ilić, R. D., Software FOTELP – Monte Carlo transport of Photonos, Electrons and Positrons; RSICC Computer Code Collection CCC-581, 1998

[15] Salvat, F., Fernandez-Vera, J. M., Baro, J., Sempau, J., PENELOPE, An Algorithm and Computer Code for Monte Carlo Simulation of Electron-Photon Showers Cimat, Centro de Investigaciones, Medioambientales y Technologicas, Technical Report No. 799, 1996

[16] Schneider, W., Bortfeld, T., Schlegel, W., Correlation Between CT Numbers and Tissue Parameters Needed for Monte Carlo Simulation of Clinical Dose Distribution, *Phys. Med. Biol.*, *45* (2000), pp. 459–478

[17] Rogers, D. W. O., Ma, C. M., Ding, G. X., Walters, B., BEAM Users Manual, NRC Report PIRS 509a, 1995

[18] Medin, J., Andreo, P., PETRA – A Monte Carlo Code for the Simulation of Proton and Electron in Water, Internal report MSF 1997-1, Karolinska Institutet, Stokholm University, 1997

[19] Ferrero, M. I., Ragona, R., Rolando, V., Sannazzari, G. L., Solano, A., Monte Carlo Simulation of a Protontherapy System for the Calculation of the Dose Distribution in a Patient, TERA 95/4 TRA 14, Fondacione per adroterapia oncologica, Novara, Italia, 1995

[20] ***, GEANT CERN Program Library Long Writeup W5013, 1994

[21] Altiparmakov, D. V., Beličev, P., An Efficiency Study of the R-Function Method Applied as Solid Modeler for Monte Carlo Calculations, *Progress in Nucl. Energy, 24* (1990), pp. 77–88

[22] Mascia, A., Schreuder, N., Ilić, R. D., Characterizing a Proton Therapy Beam with Multi Layered Faraday Cup, 2001, http://www.eps.rg/meet/HAW01/baps/abs S40058.html

[23] Paganetti, H., Gottschalk, B., Test of Monte Carlo Nuclear Interaction Model for Polyethilene (CH_2) Using Multi-Layer Faraday Cup, *Proceedings*, 44th AAPM Annual Meeting, Montreal, 2002

[24] Beebe-Wang, J. J., Dilmanion, F. A., Peggs, S. G., Schlyer, D. J., Vaska, P., Feasibility of Positron Emission Tomography of Dose Distribution in Proton-Beam Cancer Therapy, EPAC 2002, Paris, 2002

Радован Д. ИЛИЋ, Дарко ЛАЛИЋ, Србољуб Ј. СТАНКОВИЋ

СРНА – МОНТЕ КАРЛО ПРОГРАМ ЗА СИМУЛАЦИЈУ ТРАНСПОРТА ПРОТОНА У КОМБИНОВАНОЈ И ВОКСЕЛИЗОВАНОЈ ГЕОМЕТРИЈИ

У раду су описани нови Монте Карло програми за симулацију транспорта протона у комплексним геометријским облицима и материјалима различитог састава. Програм СРНА развијан је за тродимензионо (3D) рачунање расподеле дозе у протонској терапији и дозиметрији. Модел ових програма заснива се на теорији вишеструког расејања и једноставном концепту распада сложеног језгра. Пакет чине два програма: SRNA-2KG и SRNA-VOKS. Први програм симулира транспорт протона у комбинованој геометрији која може бити описана равнима и површинама другог реда. Други програм користи вокселизовану геометрију материјалних зона и он је посебно подешен за примену података компјутерске томографије. Вероватноће прелаза за оба програма припрема програм SRNADAT. Ми овде приказујемо моделе и алгоритме наших програма заједно са резултатима нумеричких експеримената нашим програмима и резултате симулације транспорта протона добијених помоћу програма PETRA и GEANT. Симулација карактеризације протонског снопа употребом вишеслојног Фарадејевог кавеза и просторне расподеле емитера позитрона добијене нашим програмом наговештава скору примену Монте Карло техника у клиничкој пракси.